2015 IEEE International Conference on Robotics and Automation (ICRA)
Washington State Convention Center
Seattle, Washington, May 26-30, 2015

Control and Energy Considerations for a Hopping Monopod on Rough Compliant Terrains

Vasileios Vasilopoulos, *Student Member, IEEE,* Iosif S. Paraskevas, *Student Member, IEEE* and Evangelos G. Papadopoulos,* *Senior Member, IEEE*

***Abstract*— Terrain compliance is a critical parameter for the performance of legged locomotion. In this work, a single actuator monopod robot hopping on rough compliant terrain is considered. Based on our controller for flat compliant terrains, this paper introduces the necessary modifications, which allow the robot to tackle the disturbance of small inclinations. Using the developed method, the robot is examined on its performance to traverse rough terrains, while maintaining the goals of reaching a desired height and forward velocity. As the increased compliance and inclination alter the energy requirements from the controller actuator, the Cost of Transport (CoT) index for a number of scenarios is studied. The correlation between terrain parameters and the CoT is presented, and useful conclusions, which can aid the understanding of the behavior of legged robots in realistic terrains are extracted.**

I. Introduction

One of the most intriguing challenges in the field of legged robotics is the development of control algorithms that render robots capable of traversing any type of terrain. However, control requirements are demanding, especially when the terrain profile is rough. An interesting approach towards running on rough terrains was introduced with the RHex robot [1], which uses open-loop control, thus forward speed is not controlled tightly. On the other hand, the BigDog robot [2], has successfully demonstrated a variety of locomotion scenarios. However its performance is highly inefficient as it uses a large internal combustion engine for its locomotion.

With these in mind, a common control strategy used by quadrupeds for traversing rough terrains involves footstep planning. LittleDog has shown impressive results on significantly uneven terrain [3]. However, it is capable only of static walking. StarlETH also uses a similar approach [4]; a foot placement algorithm along with distribution of virtual forces among the stance legs is used to overcome unexpected obstacles and external pushes and reject perturbations.

Interestingly, despite the increasing complexity of control algorithms for legged robots, many studies disregard the effect of terrain compliance and permanent deformation. For example, for the monopod hopping robot in [5], the ground was considered completely stiff. In MIT Cheetah 2, the authors determine a target ground force profile according to the desired duty cycle and stride duration, [6]. Again, the terrain is considered stiff and completely flat. On the other hand, in [7] the case of a rough terrain is considered and a control algorithm is proposed for a monopod robot on rough terrain that could handle inclinations up to 20deg. However, the robot was considered to possess two actuators, at its prismatic and rotational joint, while the main body apex height, which is crucial when running on rough terrain, was not controlled. Our recent work involved the development of a novel energy-based controller for a monopod hopping robot running over compliant terrains, using only one actuator [8].

To this end, modeling of the interaction of a legged robot with its terrain is a very important aspect for control design. Usually this is disregarded and the interaction at the stance phase is modeled as a revolute joint. However, different approaches are necessary to assess the effects of this interaction. This can be seen in works like [9], where a viscoelastic model is used, and [10], where a terradynamics approach is employed. Similar ways can be found in [11]. On the other hand, a viscoplastic model has been proposed in [8]. This approach enables one to assess the effects of terrain permanent deformations taking into account various real-life parameters such as compaction on fast dynamic walking.

In this paper, our previous work on compliant foot-terrain interaction is extended for use on rough compliant terrains. The controller presented in [8], named x-MP, is modified in order to cope with small inclinations, while the goal of the controller is again to maintain a desired apex height and speed with a single actuator. The effects of rough compliant terrain on fast dynamic walking are tackled on the expense of higher energy consumption. For this reason, the Cost of Transport criterion is used to examine how a compliant ground affects robot behavior and to extract conclusions necessary for a deeper understanding of legged locomotion on such terrains.

II. Foot-Terrain Interaction

To realistically represent the interaction of a monopod robot with the ground during running on deformable terrains, a viscoplastic impact model was proposed, [8]. The model is based on the Hunt-Crossley (HC) model [11]. According to the proposed model, the interaction force F_g at stance instance i is,

$$F_g^i\left(y_g,\dot{y}_g\right)=\begin{cases}F_c^i=\left(\lambda_c^i\cdot k_g+b_g\cdot\dot{y}_g\right)\left(y_g-y_e^{i-1}\right)^n, \dot{y}_g\geq 0\\ F_r^i=\left(\lambda_r^i\cdot k_g+b_g\cdot\dot{y}_g\right)\left(y_g-y_e^{i}\right)^n, \quad \dot{y}_g<0\end{cases} \quad (1)$$

where the subscript c stands for compression and r for restitution, y_e is the depth reached at the end of impact, k_g and b_g are the stiffness and damping coefficients respectively, n in the case of Hertzian non-adhesive contact

*Financial support by the European Union (European Social Fund-ESF) and Greek national funds through the Operational Program "Education and Lifelong Learning" of the National Strategic Reference Framework Research Funding Program: THALES: Reinforcement of the interdisciplinary and/or interinstitutional research & innovation is acknowledged.

The authors are with the Department of Mechanical Engineering, National Technical University of Athens, 9 Heroon Polytechneiou Str., 15780 Athens, Greece. (e-mail: vasilis.vasilop@gmail.com; isparas@mail.ntua.gr; egpapado@central.ntua.gr; ph.: +30-210-772-1440).

is equal to 1.5, and y_g is the depth of penetration. Note that k_g represents the equivalent stiffness between the materials that come into contact (i.e. in this case of the foot and the terrain), [12]. Damping is considered as a parameter affected by the stiffness [13], and given by

$$b_g = 1.5 \cdot c_a \cdot k_g \tag{2}$$

where c_a is usually between 0.01-0.5 depending on the materials and impact velocity. Throughout this work $c_a = 0.2$, without affecting the generality of the conclusions.

To account for successive impacts including compressions and restitutions during some leg stance, the index i is used to identify an impact instance, as the terrain inherits the characteristics from the previous impact instant due to permanent deformations. The latter are expressed with the *Coefficient of Permanent Terrain Deformation* λ, which has a recursive form

$$\lambda_c^i = \begin{cases} 1, & i = 1 \\ \lambda_r^{i-1}, & i > 1, \quad i \in \mathbb{N} \end{cases} \tag{3}$$

$$\lambda_r^i = \lambda_r^i\left(materials, velocity, i\right), \quad i \in \mathbb{N}$$

where, $\lambda_r^i \geq \lambda_c^i \geq 1$. Generally, as the same terrain point is compressed, it becomes stiffer, [8]. To model this effect, the following model was proposed for λ

$$\lambda_r^i = 1 + a(i) \cdot \left(1 - e^{-i \cdot \beta(i)}\right), \quad i \in \mathbb{N} \tag{4}$$

where $a(i)$, $\beta(i)$ are functions of the impact instance i, of the materials and of the velocity. Parameter a sets the maximum value of λ_r^i, whereas an increase in β increases the speed of reaching this value.

The final depth y_e^i at the i^{th} impact can be calculated by observing that at the maximum compression, $y_{c,\max}^i$, the following applies

$$y_{c,\max}^i \Leftrightarrow F_c^i = F_r^i \quad \text{and} \quad \dot{y}_g = 0 \tag{5}$$

Using (1), one can deduce that

$$y_e^i = y_{c,\max}^i \cdot \left(1 - \sqrt[n]{\lambda_c^i / \lambda_r^i}\right) + y_e^{i-1} \cdot \left(\sqrt[n]{\lambda_c^i / \lambda_r^i}\right) \tag{6}$$

where $y_e^0 = 0$ for consistency.

Friction. As the foot touches the ground, depending on the touchdown angle, the velocity and the materials, the foot may slip [14]. In order to assess the foot behavior during stance, a friction description is required. Here, the classical Static-plus-Coulomb model is used, as it can produce adequate results with reasonable computations, [15]. According to this model the friction force F_t is

$$F_t = \begin{cases} -\mu_c \cdot F_g \cdot \operatorname{sgn} \dot{x}_g, & \dot{x}_g \neq 0 \\ -\left|F_{\|}\right| \cdot \operatorname{sgn} F_{\|}, & \left|F_{\|}\right| < \mu_s \cdot \left|F_g\right|, \quad \dot{x}_g = 0, \quad \ddot{x}_g \neq 0 \end{cases} \tag{7}$$

where $\dot{x}_g$, $\ddot{x}_g$ are the velocity and acceleration components of the foot which are parallel to the tangential plane between the foot and the ground, F_g is the interaction force from (1) which is normal to the same tangential plane, $F_{\|}$ is the vectorial sum of all other forces applied, parallel to this tangential plane, μ_c is the Coulomb (kinetic) friction coefficient and μ_s is the static friction coefficient.

Terrain Profile Generation. To model rough terrains, a procedure has been established where a path is separated in small segments with local inclination (which can be variable or constant). One can define the length of each segment which depends on the foot characteristics - in this work twice the diameter of a $20mm$ foot has been selected as the length of each segment. This discretization leads to a simplification when the foot lies on two consecutive segments at the same time; the simulation selects the segment where the largest part of the foot lies. By increasing or decreasing the length of each segment, one can configure a desired resolution. Finally, the properties of the terrain at each point are defined by inheriting the properties of the segment they belong.

III. Monopod Robot Dynamics Model

In [8], the model of a monopod robot with a single actuator that included the description of the foot-terrain interaction was presented. However, the effect of friction was neglected and the robot was considered to run only over completely flat terrain. Here, the system model is extended by means of taking friction into account and describing the motion of the robot over rough terrain including small inclinations. The following assumptions apply: (i) the foot is a point mass thus a point contact occurs each time the foot touches the ground, (ii) bulldozing effects are neglected, (iii) the actuator is torque saturated, (iv) the pitching motion of the body is considered constrained, in accordance to the experimental setup presented in [5].

The model employed is shown in Fig. 1. It consists of a mass M describing the robot body and a mass m describing the effective mass of the robot leg and foot. The leg is springy with free length L and length at any time l, while the stiffness of the linear spring is k. The energy losses due to viscous friction in the leg prismatic degree of freedom (dof) are modeled with a damping coefficient b, while the leg angle with respect to the vertical is γ and the torque applied by the actuator at the body hip is τ.

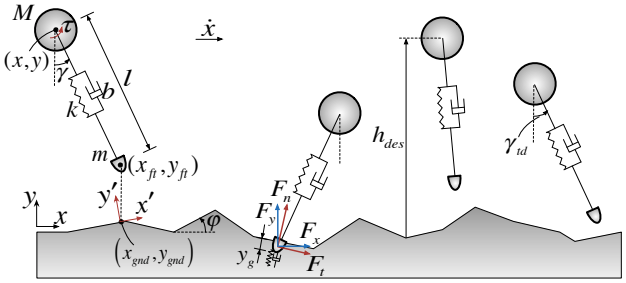

Figure 1. Model of one-legged robot on rough surface.

The system configuration for both the *flight phase*, where the foot does not touch the ground, and the *stance phase*, where the foot touches the ground, is described using the coordinates of the main body x, y and the coordinates of the foot x_{ft}, y_{ft}. The equations of motion become (with $\mathrm{s}\gamma = \sin\gamma$ and $\mathrm{c}\gamma = \cos\gamma$)

$$M \cdot \ddot{x} + k \cdot (L - l) \cdot \mathrm{s}\gamma - b \cdot \dot{l} \cdot \mathrm{s}\gamma = -\tau \cdot l^{-1} \cdot \mathrm{c}\gamma \tag{8}$$

$$M \cdot \ddot{y} + M \cdot g - k \cdot (L - l) \cdot \mathrm{c}\gamma + b \cdot \dot{l} \cdot \mathrm{c}\gamma = -\tau \cdot l^{-1} \cdot \mathrm{s}\gamma \tag{9}$$

$$m \cdot \ddot{x}_{ft} - k \cdot (L - l) \cdot \mathrm{s}\gamma + b \cdot \dot{l} \cdot \mathrm{s}\gamma = \tau \cdot l^{-1} \cdot \mathrm{c}\gamma + F_x \tag{10}$$

$$m \cdot \ddot{y}_{ft} + m \cdot g + k \cdot (L - l) \cdot \mathrm{c}\gamma - b \cdot \dot{l} \cdot \mathrm{c}\gamma = \tau \cdot l^{-1} \cdot \mathrm{s}\gamma + F_y \tag{11}$$

where F_x, F_y are the ground forces in the horizontal and vertical direction respectively, defined in the inertial frame.

These forces are determined from the normal and tangential components of the interaction force with respect to the common tangential plane between the foot mass and the ground, F_n and F_t, using the terrain inclination φ, as

$$F_x = -F_n \cdot \sin\varphi + F_t \cdot \cos\varphi \quad (12)$$

$$F_y = F_n \cdot \cos\varphi + F_t \cdot \sin\varphi \quad (13)$$

To implement the viscoplastic contact model and calculate friction, the foot position and velocity in the normal and the tangential directions must be calculated. For this reason, a local coordinate system (x', y') is defined with axes tangential and normal to the ground surface correspondingly. The origin of this system during the flight phase is always located at the point (x_{gnd}, y_{gnd}) of the terrain profile that is just below the horizontal foot position, as shown in Fig 1. During the stance phase, the origin of the system remains coincident with the point where the collision with the ground occurred. In this way, the foot position is being calculated in the local coordinate system using the following transformation from the inertial coordinate system

$$\mathbf{r}' = \mathbf{T} \cdot \mathbf{r} \quad (14)$$

where $\mathbf{r}' = [\ x'_{ft} \quad y'_{ft} \quad 0 \quad 1\ ]^T$ contains the foot position in the local coordinate system, $\mathbf{r} = [\ x_{ft} \quad y_{ft} \quad 0 \quad 1\ ]^T$ contains the foot position in the inertial coordinate system and $\mathbf{T}$ is the transformation matrix from the inertial to the local coordinate system given as

$$\mathbf{T} = \begin{bmatrix} \cos\varphi & \sin\varphi & 0 & -x_{gnd}\cdot\cos\varphi - y_{gnd}\cdot\sin\varphi \\ -\sin\varphi & \cos\varphi & 0 & x_{gnd}\cdot\sin\varphi - y_{gnd}\cdot\cos\varphi \\ 0 & 0 & 1 & 0 \\ 0 & 0 & 0 & 1 \end{bmatrix} \quad (15)$$

Using (14), the foot velocity components in the normal and tangential directions $\dot{x}'_{ft}$, $\dot{y}'_{ft}$ are also determined as follows

$$\dot{x}'_{ft} = \dot{x}_{ft} \cdot \cos\varphi + \dot{y}_{ft} \cdot \sin\varphi \quad (16)$$

$$\dot{y}'_{ft} = -\dot{x}_{ft} \cdot \sin\varphi + \dot{y}_{ft} \cdot \cos\varphi \quad (17)$$

Based on assumption (i) and on the former analysis, the ground penetration depth y_g equals the foot position y'_{ft} in the local system during stance, see Fig. 1. Therefore, y'_{ft}, $\dot{y}'_{ft}$ substitute y_g, $\dot{y}_g$ in (1), while $\dot{x}'_{ft}$ substitutes $\dot{x}_g$ in (7). The stance phase begins with the foot initially touching the ground following a flight phase $(y'_{ft} = 0)$ and terminates when the ground force is zeroed $(F_n = 0)$. During flight, the forces from the ground are zero $(F_n, F_t = 0)$.

IV. Control Methodology

In [8], a novel controller called *Extended Multipart (x-MP)* was presented. The controller is capable of achieving and retaining a desired forward speed and main body apex height on any terrain described by the viscoplastic contact model, with a single actuator located at the robot hip. This controller uses energy principles and does not require an estimate of the terrain properties. However, its implementation is limited to completely flat terrains with no inclination. In this paper the x-MP is extended to achieve hopping on rough terrains with small inclinations of $\pm 5\,\text{deg}$. Larger inclinations would require higher torques to avoid motor saturation.

The controller in this work is applied just after each liftoff of the leg, when the stance phase of stride $j-1$ terminates and the flight phase of stride j begins. At that moment, it calculates a desired touchdown angle γ_{td}^j for stride j and a constant torque τ_s^j to be applied during the stance phase of stride j. The controller performs its calculations in three steps, as described in the following section.

Step 1 - Prediction of next touchdown ground point. The first action of the controller is to predict the point of the ground surface on which the leg touchdown of stride j will occur. In general the terrain profile is described by a function $y_{gnd} = f(x_{gnd})$ which is unknown to the robot. By estimating the next touchdown point, the control algorithms developed for flat terrain can then be applied. The basic idea for this estimation is depicted in Fig. 2, where the touchdown instants of strides $j-2$ and $j-1$, as well as the estimated touchdown instant of stride j are shown.

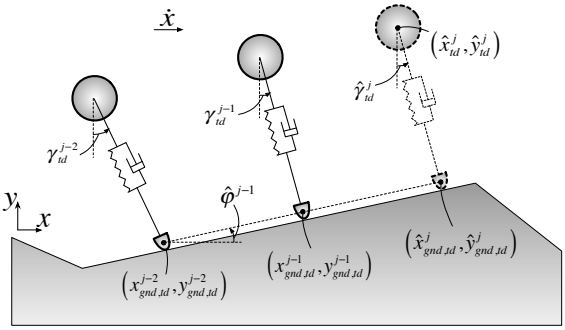

Figure 2. Touchdown ground point estimation algorithm concept.

To be more specific, after each touchdown of the robot leg, the terrain profile coordinates $x_{gnd,td}$ and $y_{gnd,td}$ at that point are calculated using the following kinematic equations

$$x_{gnd,td} = x_{ft,td} = x_{td} + l_{td} \cdot \sin\gamma_{td} \quad (18)$$

$$y_{gnd,td} = y_{ft,td} = y_{td} - l_{td} \cdot \cos\gamma_{td} \quad (19)$$

where the subscript 'td' denotes the value of each magnitude at touchdown. Relying on the response of the previous two strides and using (18) and (19), the controller estimates the terrain inclination of the stride $j-1$ as follows

$$\hat{\varphi}^{j-1} = \tan^{-1}\left(\frac{y_{gnd,td}^{j-1} - y_{gnd,td}^{j-2}}{x_{gnd,td}^{j-1} - x_{gnd,td}^{j-2}}\right) \quad (20)$$

with $(\hat{\#})$ denoting an estimated magnitude of $(\#)$. For the first and the second stride where no previous data exists, $\hat{\varphi}^0 = \hat{\varphi}^1 = 0$.

Next, the following assumptions are made for stride j: (i) due to small length strides, like those examined in this work, the terrain inclination will remain the same, (ii) the touchdown angle will be approximated as being equal to the touchdown angle during stride $j-1$ so that $\hat{\gamma}_{td}^j \approx \gamma_{td}^{j-1}$ and (iii) the robot main body performs a ballistic trajectory during flight. The goal is to estimate the touchdown point $\left(\hat{x}_{gnd,td}^j, \hat{y}_{gnd,td}^j\right)$ of the terrain profile. Using assumptions (ii) and (iii), the following set of equations can be formed regarding the ballistic trajectory of the robot main body

$$\hat{y}_{td}^j = \hat{y}_{gnd,td}^j + L \cdot \cos\hat{\gamma}_{td}^j = y_{lo}^{j-1} + \dot{y}_{lo}^{j-1} \cdot \Delta\hat{t}_f^{\,j} - 0.5g \cdot \left(\Delta\hat{t}_f^{\,j}\right)^2 \quad (21)$$

$$\hat{x}_{td}^j = \hat{x}_{gnd,td}^j - L \cdot \sin\hat{\gamma}_{td}^j = x_{lo}^{j-1} + \dot{x}_{lo}^{j-1} \cdot \Delta\hat{t}_f^{\,j} \quad (22)$$

with the subscript 'lo' denoting the value of each magnitude at liftoff and $\Delta\hat{t}_f^{\,j}$ the estimated duration of flight for the stride j. Using assumption (i), $\hat{x}_{gnd,td}^j$ and $\hat{y}_{gnd,td}^j$ are related according to the following equation

$$\hat{y}^{j}_{gnd,td} = y^{j-1}_{gnd,td} + \left(\hat{x}^{j}_{gnd,td} - x^{j-1}_{gnd,td}\right)\cdot \tan\hat{\varphi}^{j-1} \quad (23)$$

Equations (21), (22) and (23) formulate a 3x3 system, with $(\hat{x}^{j}_{gnd,td}, \hat{y}^{j}_{gnd,td}, \Delta\hat{t}^{j}_{f})$ being the unknown variables. This system can be analytically solved and yield the estimated point $(\hat{x}^{j}_{gnd,td}, \hat{y}^{j}_{gnd,td})$.

Step 2 - Calculation of desired touchdown angle. After the calculation of $\left(\hat{x}^{j}_{gnd,td}, \hat{y}^{j}_{gnd,td}\right)$, the controller calculates the desired touchdown angle γ^{j}_{td}. In [8], a method was proposed where the extended robot model describing the foot-terrain interaction could be mapped to a simple model for stiff terrains by calculating an equivalent stiffness and damping k' and b' respectively, as shown in Fig. 3. The calculation of k', b' was made using previous stride response and calculating the energy losses due to damping and ground dissipation. The desired touchdown angle γ^{j}_{td} was determined by integrating the flight and stance dynamics of the equivalent simple model, according to the desired main body apex height h_{des}.

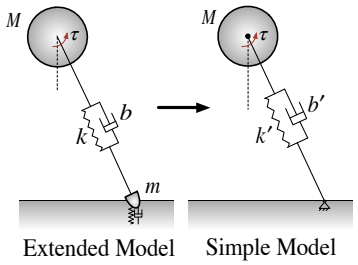

Figure 3. Idea of the x-MP controller.

The same control approach is used here, with the main difference that the ground level is now considered to be at $\hat{y}^{j}_{gnd,td}$ rather than at zero and the desired main body apex height is determined so that a specific clearance from the ground $\Delta h_{cl,des}$ is reached, as follows

$$h_{des} = \Delta h_{cl,des} + \hat{y}^{j}_{gnd,td} \quad (24)$$

Step 3 - Calculation of constant stance torque. Following the calculation of the desired touchdown angle, the x-MP determines a constant torque τ^{j}_{s} to be applied during the next stance phase. This torque is calculated so that a desired energy level is reached [8]. The controller has to compensate for leg damping energy losses and energy losses due to ground dissipation, as well as accelerating or decelerating the system according to the desired forward velocity $\dot{x}_{des}$ and apex height h_{des}. The same algorithm is used here.

Following these calculations, the leg is servoed to the desired touchdown angle γ^{j}_{td} during the flight phase using a PD controller as described in [8]. After the leg touchdown, which is determined using a force sensor at the robot foot, the constant torque τ^{j}_{s} is applied.

Discussion. The controller uses information from a force sensor yielding the ground reaction forces (F_n, F_t) and from two encoders that measure the leg angle γ and the leg length l, and estimates the body position (x,y) using the robot dynamic model fused with data from an inertial sensor, [8]. No extra sensor for determining the terrain properties or inclination is required. Finally, the controller does not need tuning since it does not use any tunable gains; it just requires an estimate of the robot parameters.

V. Results

To evaluate the controller and extract conclusions about energy requirement issues under different scenarios, various simulation scenarios were run. The equivalent stiffness k_g between the materials in contact (i.e. foot and ground) was used [12], where the properties of various terrains were found in [16]. In this work an ether polyurethane foot was considered with Young's modulus $E = 100\text{MPa}$. As an example, the equivalent stiffness between this material and granite with Young's modulus $E = 50\text{GPa}$ is $k_g \approx 450{,}000\,\text{N/m}$. In this way, three main categories of terrains were examined: *soft* ground with $k_g = 8\cdot 10^4\,\text{N/m}$, $\mu_s = 0.5$ and $\mu_c = 0.4$, *moderate* ground with $k_g = 2\cdot 10^5\,\text{N/m}$, $\mu_s = 0.6$ and $\mu_c = 0.5$, and *stiff* ground with $k_g = 4\cdot 10^5\,\text{N/m}$, $\mu_s = 0.7$ and $\mu_c = 0.6$.

In all cases, a monopod was considered with parameters: $M = 4\text{kg}$, $m = 0.1\text{kg}$, leg length $L = 0.30\text{m}$, and spring and damper parameters $k = 12{,}000\text{N/m}$ and $b = 3\text{Ns/m}$. The acceleration of gravity was $9.81\,\text{m/s}^2$. The simulations were performed in Matlab using ode23s with absolute and relative tolerance 10^{-2} and maximum step 10^{-5}. To minimize the zero-crossing arithmetic problems created by the numerical stiffness, the impact was considered over when the interaction force between the foot and the terrain was below 5N, while the foot transition from slip to stick occurred when the foot horizontal velocity was below $10^{-4}\,\text{m/s}$ (by increasing tolerances, these values can be lower, however this set was selected as it produced both fast and reasonable results after examining various sets of tolerances).

Performance of the controller on rough terrain. In Fig. 4 the response of the controller on a rough terrain profile with maximum inclination of $\pm 2\,\text{deg}$ is shown. The initial conditions were: height $h_0 = 0.32\text{m}$, forward velocity $\dot{x}_0 = 0.6\,\text{m/s}$. The desired commands were clearance from the ground $\Delta h_{cl,des} = 0.32m$ and forward velocity $\dot{x}_{des} = 0.6\,\text{m/s}$, while the ground was considered stiff. The simulations showed that the controller retained the desired forward velocity and followed smoothly the desired apex height profile, using the touchdown ground point estimation algorithm presented here.

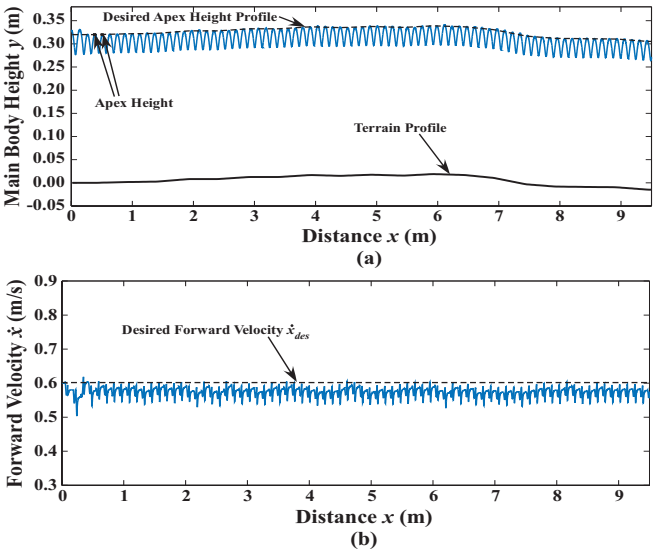

Figure 4. Controller performance on rough, random-generated terrain profile: (a) Main Body Height, (b) Forward Velocity.

Moreover, a different scenario was considered where the profile resembles a shallow crater with maximum inclination of $\pm 3\text{deg}$, as shown in Fig. 5. At each part of the designated path, the contact stiffness and shape deformation (shown by the max $\lambda = \left[1 + a(i)\right]$ in the figure) were also changed. The initial conditions and desired magnitudes remained the same as the previous scenario. The controller adapted quickly to each terrain and followed the desired objectives of forward velocity and main body height, as it is shown in Fig 5 and in the accompanying video.

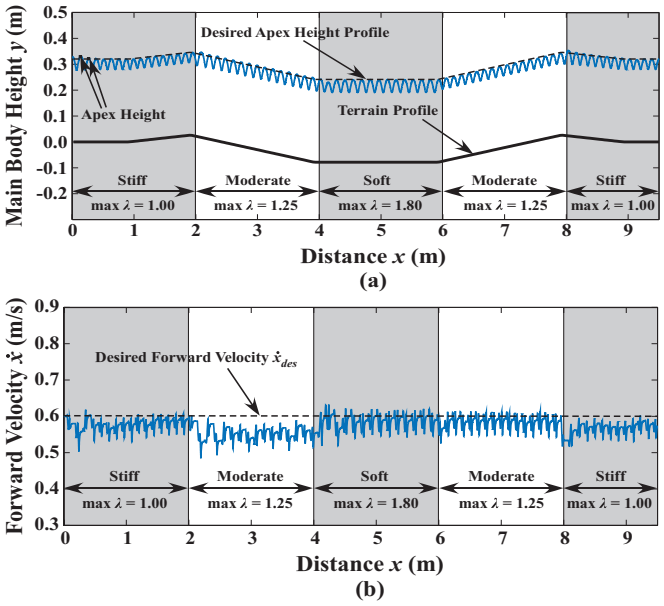

Figure 5. Controller performance on a crater-like terrain profile: (a) Main body height, (b) Forward velocity.

Note that the response converges more slowly to the desired commands when the robot runs downhill. This is due to the fact that the flight phase duration is larger; in this way, there are less touchdowns for the same horizontal distance and the constant stance torque, which is the control input that regulates the system energy level, is applied less frequently.

Except for the controller performance, it is interesting to examine the controller behavior, as the environment becomes more demanding. For this reason, in Fig. 6, the leg angle response and the commanded constant torques for the various stance phases of the motion depicted in Fig. 5 are shown. It must be noted that negative torque corresponds to positive work, since the leg moves in the negative direction during stance, which is desired. As can be seen, on the uphills, the controller set larger touchdown angles and constant torques in order to retain the desired forward velocity. On the contrary, when the robot ran downhill, the controller tried to decelerate the body and cancel the gravity effect; for this reason the touchdown angles and the constant torques were smaller in comparison to the uphill or flat motion. The constant torques on the downhills were mostly positive; this is due to the fact that the controller subtracted energy from the system and tried to decelerate it. This behavior of the controller is verified by many examples in nature, i.e when a human runs uphill and tries to retain a forward speed, larger leg angles and greater effort are required, whereas when running downhill, humans try to cancel the effect of gravity by applying smaller leg angles and decelerating. The controller outputs also depended on terrain properties. The more compliant and with larger deformations was the ground, the larger touchdown angles and stance torques were.

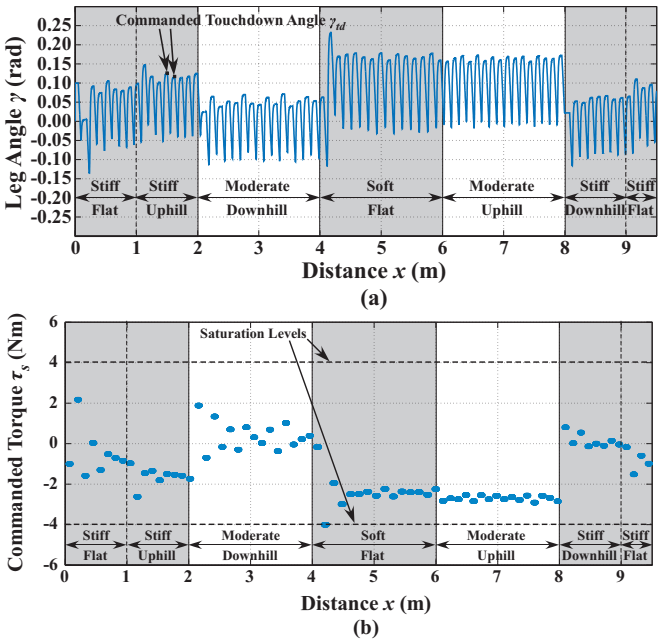

Figure 6. (a) Leg angle response and (b) Constant torque commanded by the controller, for the motion of the robot on crater-like terrain profile.

Energy Requirements and Cost of Transport. It is interesting to examine the energy requirements for different motion scenarios. For this reason, the Cost of Transport (CoT) index was used, which is defined as follows

$$CoT = W / \left[(M+m) \cdot g \cdot d \right] \tag{25}$$

where W is the total work over a distance d. Note that no regenerative braking was assumed so that, except for positive work W^+, negative work W^- was also considered in the calculation of total work W as follows

$$W = W^+ + \left| W^- \right| \tag{26}$$

By using the CoT index, useful insights on the parameters that affect the motion of legged robots and the commands that lead to lower energy levels were identified. Eventually such kind of analyses can lead to methods of determining their optimal gait that corresponds to specific terrain characteristics and required objectives.

In Fig. 7a the effect of terrain inclination on CoT for different forward velocities is presented. The ground was considered stiff with no permanent deformation $(\lambda = 1)$. It can be seen that the value of CoT mainly depended on the terrain inclination rather than the forward velocity. Also, negative inclinations resulted in less energy consumption by the actuator than positive inclinations of the same absolute value, since gravity helped the robot to achieve its objectives when running downhill. However, the minimum CoT was achieved for an inclination around $-2\,\text{deg}$, whereas for steeper downhill the CoT increased again as the actuator spent additional energy to decelerate the robot and cancel the effect of gravity. It could be, therefore, suggested that there may be an inclination value around $-2\,\text{deg}$, where a passive gait could be preserved without any actuation, should there be no energy losses due to impact with the ground.

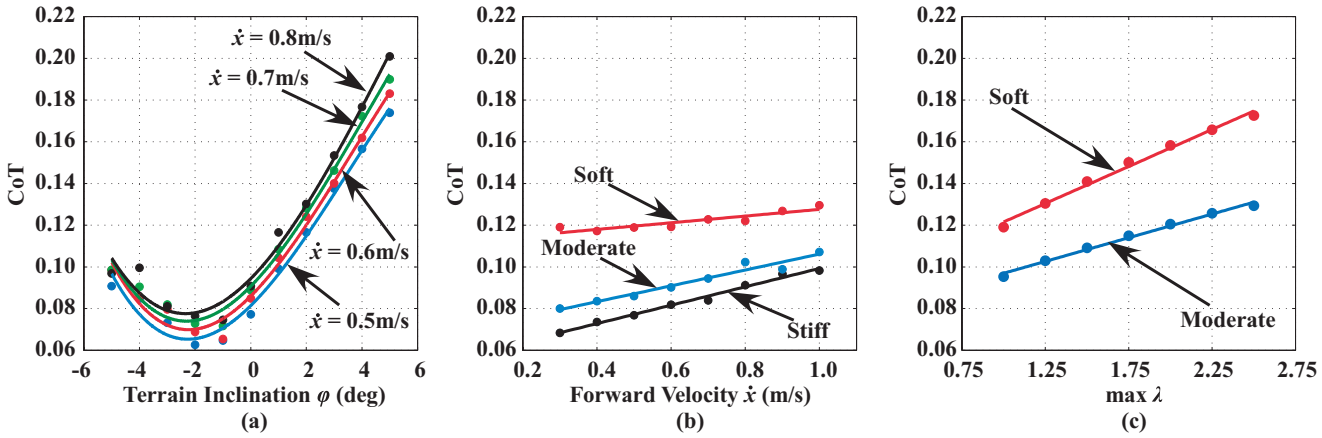

Figure 7. Dependence of CoT: (a) On different inclinations for stiff terrain and various velocities, (b) On various velocities for different terrain types with no permanent deformation and (c) On permanent deformations for compliant terrains with 0.6m/s desired velocity.

In Fig. 7b, the effect of forward velocity on CoT for different terrains is shown. The ground was considered flat with no permanent deformation $(\lambda = 1)$. It can be seen that the CoT increased as the ground became more compliant. This seems reasonable according to physical understanding, as for example running on clay requires extra effort than running on concrete. Additionally, the CoT increased linearly with the forward velocity due to the fact that greater running speed resulted in impacts with greater energy losses, which the controller had to compensate in order to maintain the robot motion. This leads to the conclusion that passive motions are difficult to be retained on real terrains, not only due to robot mechanical damping but also due to energy losses at the impact with the ground. Moreover the effect of forward velocity on the CoT became less significant as the ground became more compliant, as the inclination of the fitting lines gradually decreased. This leads to the conclusion that ground compliance is more important than desired forward velocity when designing a controller for significantly rough and/or compliant terrains.

Finally in Fig. 7c the effect of permanent deformations on the CoT when running on terrains that can be permanently deformed is shown. The ground was considered flat and a forward velocity of 0.6m/s was retained. The CoT increased linearly with λ, which shows the significance of permanent deformations. Also, the effect of permanent deformations becomes more important as ground compliance increases.

VI. Conclusion

In our previous work the importance of taking into account the terrain compliance during the hopping of a monopod robot with a single actuator has been established and a control method was proposed, named x-MP. In this work, this controller was extended in order to achieve apex height and forward velocity control on rough terrains, which are modeled as terrains with disturbances in the form of small inclinations. A theoretical analysis has been presented and the corresponding algorithm has been developed and demonstrated. Simulations proved the validity of the concept. The energy consumption on compliant terrains has been studied by means of various scenarios which included stiff, moderate and soft terrains with or without small inclinations and with different degree of compliance. The results were in line with our physical experience, and the dependence of the CoT on inclination, terrain and speed was also studied and discussed yielding interesting results.

References

[1] Saranli, U., Buehler, M. and Koditschek, D.E., "RHex: A Simple and Highly Mobile Hexapod Robot", *The Int. Journal of Robotics Research*, vol. 20, pp. 616-631, 2001.

[2] Buehler, M., Playter, R. and Raibert, M., "Robots Step Outside", in *Int. Symp. Adaptive Motion of Animals and Machines*, Ilmenau, 2005.

[3] Kalakrishnan, K. et al, "Fast Robust Quadruped Locomotion over Challenging Terrain", *IEEE Int. Conf. on Robotics and Automation (ICRA '10)*, May 2010, Anchorage, Alaska, USA, pp. 2665-2670.

[4] Gehring, C. et al, "Control of Dynamic Gaits for a Quadrupedal Robot", *IEEE Int. Conf. on Robotics and Automation* (ICRA '13), May 2013, Karlsruhe, Germany, pp. 3287-3292.

[5] Cherouveim, N. and Papadopoulos, E., "Control of Hopping Speed and Height Over Unknown Rough Terrain Using a Single Actuator," *IEEE Int. Conf. on Robotics and Automation* (ICRA '09), Kobe, Japan, May 2009, pp. 2743-2748.

[6] Park, H., et al., "Quadruped Bounding Control with Variable Duty Cycle via Vertical Impulse Scaling," *IEEE/RSJ Int. Conf. on Intelligent Robots and Systems* (IROS), Chicago, Illinois, USA, 2014, pp. 3245–3252.

[7] Faraji, S. et al, "Compliant and Adaptive Control of a planar monopod hopper in rough terrain", *IEEE Int. Conf. on Robotics and Automation* (ICRA '13), Karlsruhe, Germany, May 2013, pp. 4818-4825.

[8] Vasilopoulos, V., Paraskevas, I. S. and Papadopoulos, E. G., "Compliant Terrain Legged Locomotion Using a Viscoplastic Approach", *IEEE/RSJ Int. Conf. on Intelligent Robots and Systems* (IROS '14), Chicago, Illinois, USA, September 2014, pp. 4849-4854.

[9] Wu, A., and Geyer, H., "Highly Robust Running of Articulated Bipeds in Unobserved Terrain," *IEEE/RSJ Int. Conf. on Intelligent Robots and Systems*, Chicago, Illinois, USA, 2014, pp. 2558–2565.

[10] Li, C., Zhang, T., and Goldman, D.I., "A terradynamics of legged locomotion on granular media," *Science*, 339(6126), pp. 1408-1412, 2013.

[11] Gilardi, G. and Sharf, I., "Literature Survey of Contact Dynamics Modelling," *Mechanism & Machine Th.*, 37(10), pp. 1213-1239, 2002.

[12] Johnson, K. L., *Contact mechanics,* Cambridge Univ. Press, 1977.

[13] Marhefka, D. W. and Orin, D. E., "A compliant contact model with nonlinear damping for simulation of robotic systems," *IEEE Transactions on Systems, Man, and Cybernetics-part A: Systems and Humans*, vol. 29, no. 6, pp. 566-572, 1999.

[14] Stronge, W. J., *Impact Mechanics*, Cambridge Univ. Press, 2000.

[15] Papadopoulos, E. G., and Chasparis, G. C., "Analysis and Model-Based Control of Servomechanisms With Friction," *J. Dynamic Systems, Measurement, and Control,* 126(4), pp. 911-915, 2004.

[16] Zhu, T., "Some Useful Numbers on the Engineering Properties of Materials", [online], http://goo.gl/pY8jeK (Acc.: 4 February 2015).